www.czasopisma.pan.pl PAN POLSKA AKADEMIA NAUK www.journals.pan.pl

BULLETIN OF THE POLISH ACADEMY OF SCIENCES
TECHNICAL SCIENCES, Vol. 60, No. 3, 2012
DOI: 10.2478/v10175-012-0071-0

Tool stiffness influence on the chosen physical parameters of the milling process

W. ZĘBALA*

Production Engineering Institute, Cracow University of Technology, 37 Jana Pawła II Ave., 31-864 Kraków, Poland

Abstract. This article presents our own model researches, relating to the down milling process of Aluminium alloy (Al6061) and Titanium alloy (Ti6Al4V), with a tool made of sintered carbides. These investigations pay the special attention to the impact of the tool rigidity on the process of chip formation. The simulation calculations have been carried out for two cases of the cutting process: case 1 – assuming an ideally rigid construction of a milling cutter (length of tool does not impact its deflection under the cutting forces); case 2 – it is possible that the tool can be subjected to deflection under the cutting forces (length of a tool part is counted from the holder end to the contact point of a cutting edge with the machining material).

Key words: stiffness, milling, modelling.

1. Introduction

Rigidity is understood as a property of the structural element, which consists in opposing the deformations caused by the loads acting on such an element. Rigidity decisively impacts the shape and surface roughness of the object being worked [1–3]. It is also essentially important for the process of the chip formation and life of the tool edge [4, 5]. Directions of deformations do not have identical impact on the accuracy of shape and dimensions. The greatest changes in the dimensions and shape are caused by such forces which act perpendicularly to the machined surface [2, 6]. A measure of the linear rigidity of the element (static rigidity) is the proportion of the force F_i to the deformations f_i caused by such a force (1):

$$j_i = \frac{F_i}{f_i} \quad \text{[N/mm]}. \tag{1}$$

The inverse ratio is called a workability. Looking into some specific system consisting of a machine tool – chuck – work piece - tool (*MCWT*) it is most conveniently to take into consideration the dislocations of x, y, z within the machine tool adopted system of coordinates, and relating rigidities j_x, j_y, j_z, in the direction of forces F_x, F_y, F_z action. In the case of angular rigidity, proportion of the twisting moment M_s to the resultant angular deformation ϕ is taken into consideration (2).

$$j_M = \frac{M_s}{\varphi} \quad \text{[Nm/degree]}. \tag{2}$$

Generally speaking about the rigidity, we usually have in mind the complete *MCWT* system, so we take into account the relative displacement, which occurs in the place of the tool contact with the object, in result of elastic deformation of the *MCWT* system by the resultant force F [7–10]. We can also separately consider the rigidity of the individual elements included in the *MCWT* system. In such a case, we determine rigidity of the tool, object and individual structural elements of the machine-tool (e.g., carriage, tool holder, spindle, etc.).

Rigidity of the tool is closely connected with its construction (shape and dimensions), rigidity of fastening elements and additional supports. Some tools are highly susceptible to deformations, e.g., most of tools used in processing of holes, in particular the deep-hole drills or shank-type milling cutters [11, 12]. In order to minimize the influence of the tool susceptibility to machining error, drill bushes are used (Fig. 1), rests as well as the suitable selection of the cutting parameters and the tool edge geometry (reduction of the component values of the total cutting force).

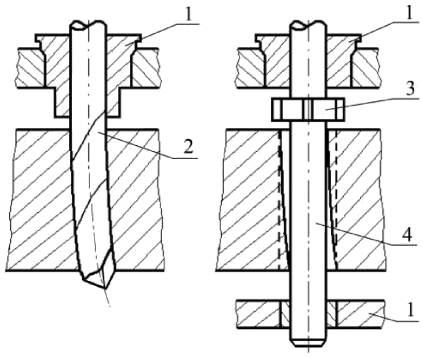

Fig. 1. Reducing the susceptibility of the tools (acc. to Storch, Ref.12)
Indications: 1, 3 – leading bushes, 2, 4 – tools

The tool static rigidity performs a significant role in the two principal cases [1, 2, 13]:

1. When the tool is a prevailing component of the discussed *MCWT* system, and because of that, its rigidity directly impacts the machining process (e.g., vibrations).
2. When deformation of the tool directly impacts geometrical accuracy of the machining (shape errors of the worked object).

*e-mail: zebala@mech.pk.edu.pl

Knowledge of the acting static loads and the static susceptibility of the *MCWT* system, does not allow to predict its reaction in the dynamic working conditions. It is, however, possible to estimate an order of magnitude of such deviations being consequence of the manufacturing errors. The example two-dimensional dynamic model of the machining process according to Stépán [3] is presented in Fig. 2.

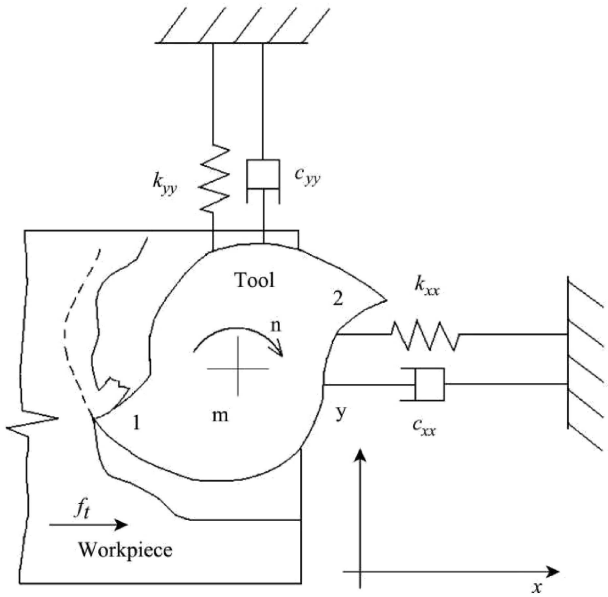

Fig. 2. Two-dimensional model of cutting process (acc. to Stépán, Ref. 3)

In Fig. 3 a schematic drawing of a tool holder is presented together with a milling cutter held in it. The tool projects from the holder to the length L:

$$L = L_1 + L_2, \tag{3}$$

where L_1 indicates free length of the tool measured from the holder end to the point of contact of the tool edge with the work piece material, L_2 is the length of the milling cutter part, sunk into the material (axial depth of cut a_p).

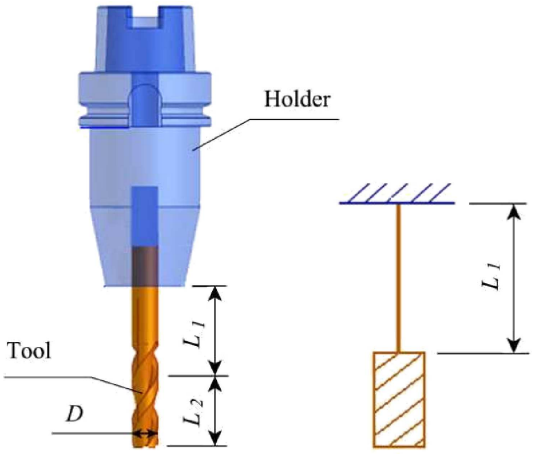

Fig. 3. Drawing of the mounting tool holder: D – tool diameter, L_1 – free length of the tool measured from the holder end to the point of contact of the tool edge with the work piece material

In the case of the rigidly mounted beam (shank cutter) (Fig. 4), with length L_1 and the constant cross-section, we can calculate displacement of the tool axis y (deflection) at the place of the loading force F action, from the formula (4), (5). An example of the influence of the loading force value F and the free length of the tool L_1 on the tool deflection y is presented in Fig. 5.

$$y = \frac{FL_1^3}{3EJ}, \tag{4}$$

$$J = \frac{\pi D^4}{64}, \tag{5}$$

where J – geometrical moment of inertia of the surface for a cylinder with diameter D, E – Modulus of elasticity.

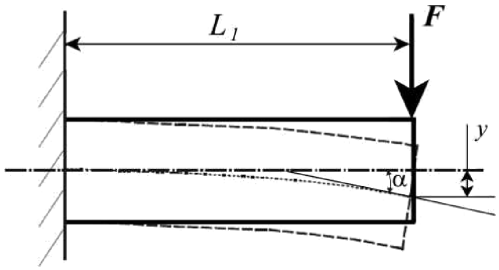

Fig. 4. Displacement of the tool axis at the place of the loading force F action

a)

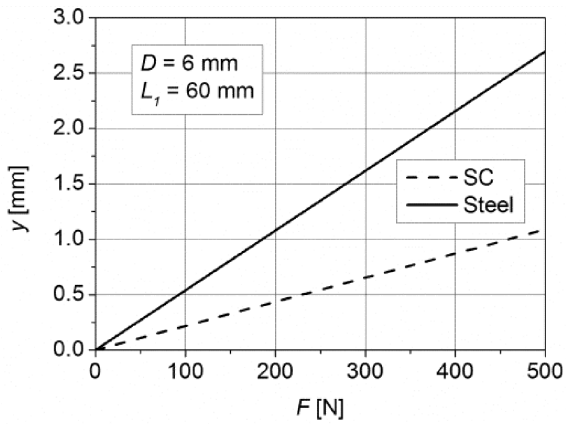

b)

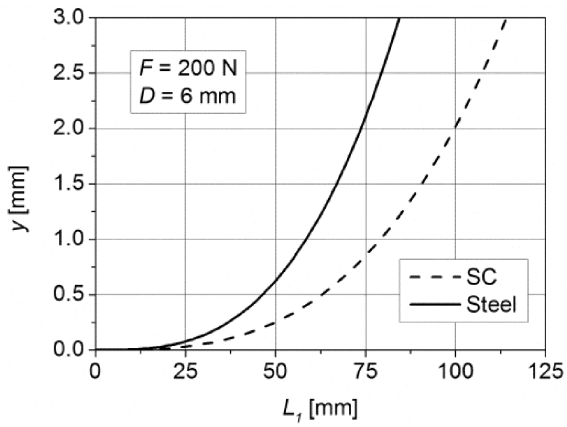

Fig. 5. The influence of the loading force value F and the free length of the tool L_1 on the size of tool deflection for sintered carbide (SC) and steel

In very complex loading conditions not only amplitude varies but also the loading direction [14]. Additionally, introduction the radial deviation to the deformable object, even of a small value, increases significantly the magnitude of the equivalent stress [15].

A relative displacement of the cutting edge (in the direction of the axes x, y, z) occurs in the place of contact of the working part of the milling cutter with the work piece material, as an effect of elastic deformation [6] (Fig. 6). Such displacement can be either the effect of the tool deflection or the dislocation of the milling cutter axis, resulting from the non-rigid fastening of the tool in the tool holder.

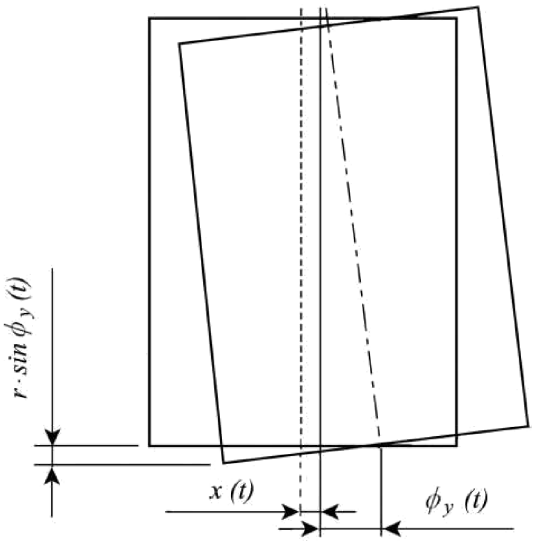

Fig. 6. Displacement of tool axis as the effect of elastic deformation (acc. to Szalay, after Ref. 6)

2. Modelling of the milling process with the regard to the static rigidity of the tool

A model of the milling process, with the regard to the static rigidity of the tool is presented in Fig. 7 (the maximum number of finite elements was 120000). Simulation of the machining process was carried out for the process of the down milling of the Aluminium alloy (Al 6061) and the Titanium alloy (Ti6Al4V). Cutting parameters and geometrical dimensions of the tool are set in Table 1. Numerical computation was carried out basing on the three-dimensional Lagrangian finite element method [16]. Techniques such as adaptive remeshing, explicit dynamics and tightly coupled transient thermal analysis were integrated to model the complex interactions of the cutting tool (wedge) and work piece. Equation (6) presents the constitutive model by which the material is governed.

$$\sigma(\varepsilon^p, \dot{\varepsilon}, T) = g(\varepsilon^p) * \Gamma(\dot{\varepsilon}) * \Theta(T), \tag{6}$$

where $g(\varepsilon^p)$ is strain hardening, $\Gamma(\dot{\varepsilon})$ is strain rate sensitivity and $\Theta(T)$ is thermal softening.

a)

b)

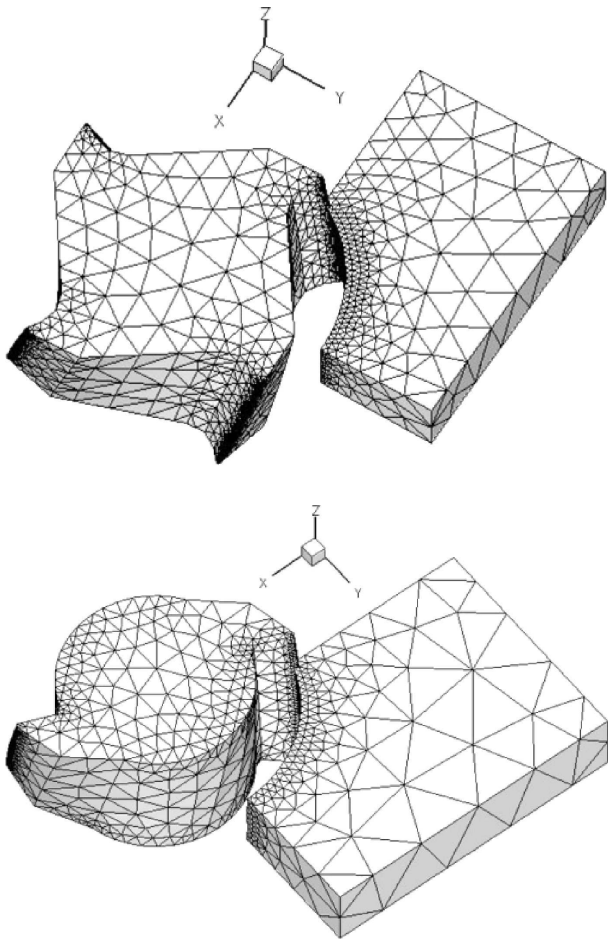

Fig. 7. Model of milling process with the finite element net for the work piece material: a) Aluminium alloy, b) Titanium alloy

Table 1
Cutting parameters and the geometrical tool dimensions

Work piece material	Length of tool L_1 [mm]	Diameter of tool D [mm]	f_z [mm/tooth]	v_c [m/min]	a_e [mm]	a_p [mm]
Al6061	0	8	0.15	500	2	1
	100					
	200					
Ti6Al4V	0	6		90		
	60					

In the simulation of the Aluminium alloy milling process a four-edge shank-type milling cutter was used, while in the case of the Titanium alloy, the two-edge milling cutter was applied. Results of the numerical computations carried out, in the form of elastic deformations of the machined layer and displacement of the cutting edge during the process of machining, distribution of temperature within the machining area and the course of the main cutting force components are presented in Figs. 8–12 (for Aluminium alloy) and Figs. 13–16 (for Titanium alloy).

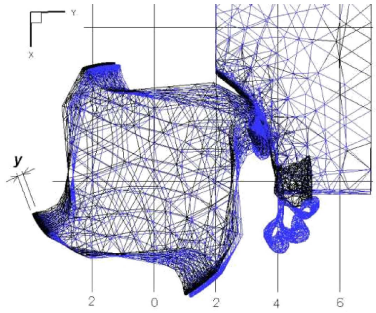

Fig. 8. Model of the cutting process of the Aluminium alloy with a plot of finite elements before (blue colour) and after the deformation (black colour)

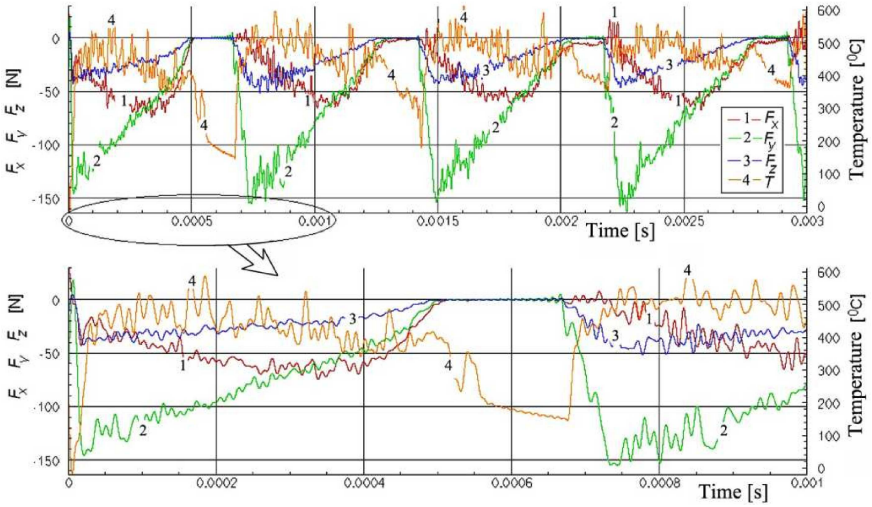

Fig. 9. Graph of the course of the main cutting force components (F_x, F_y, F_z) and the maximum temperature of the edge ($T_{\max}$) during down milling of Aluminium alloy Al 6061, assuming fully rigid construction of the tool (beam length $L_1 = 0$ mm)

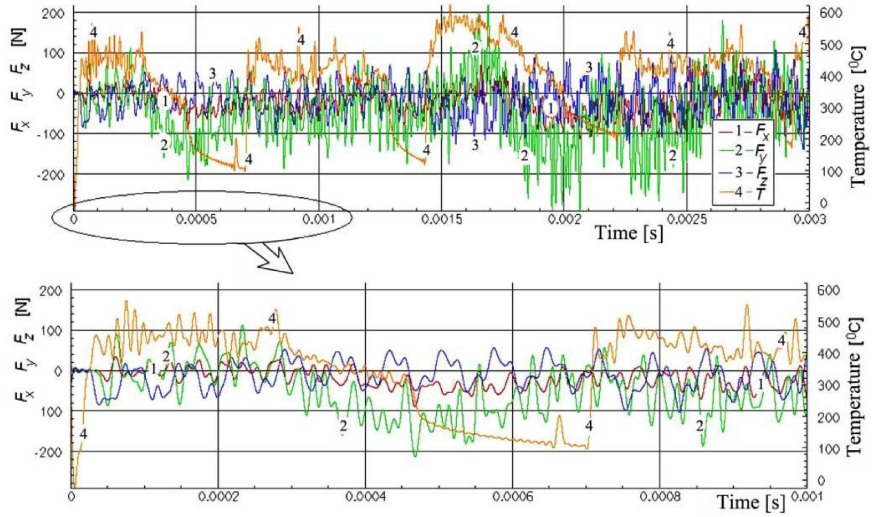

Fig. 10. Graph of the course of the main cutting force components (F_x, F_y, F_z) and the maximum temperature of the edge ($T_{\max}$) during down milling of Aluminium alloy Al 6061, with the rigidity, determined by the free length of the tool (beam) with length $L_1 = 100$ mm

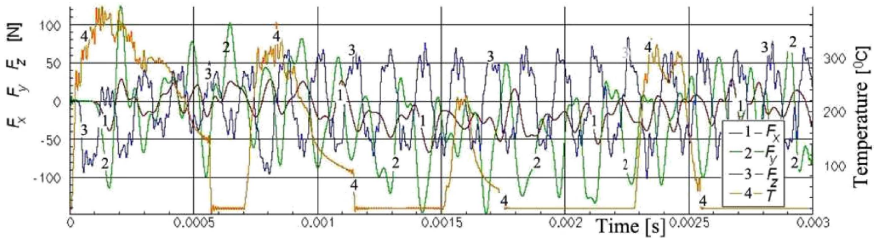

Fig. 11. Graph of the course of the main cutting force components (F_x, F_y, F_z) and the maximum temperature of the edge ($T_{\max}$) during down milling of Aluminium alloy Al 6061, with the rigidity, determined by the free length of the tool (beam) with length $L_1 = 200$ mm

a)

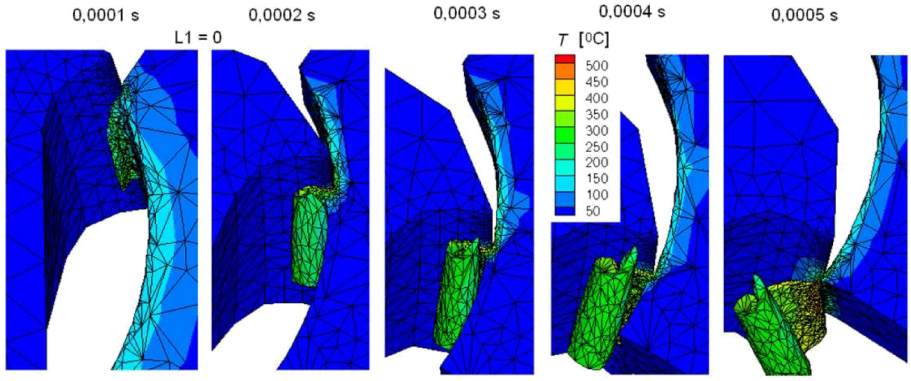

b)

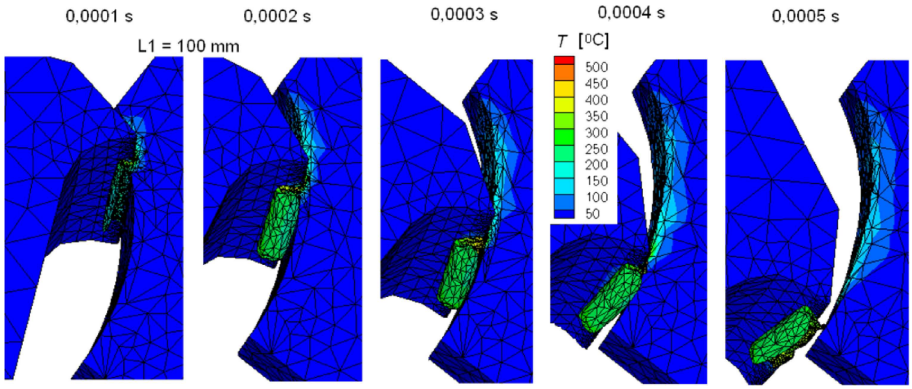

Fig. 12. Subsequent stages of the chip formation during the down milling of Aluminum alloy Al 6061 in the case of: a) the full rigidity of the tool, b) the rigidity, determined by the free length of the tool (beam) with length $L_1 = 100$ mm

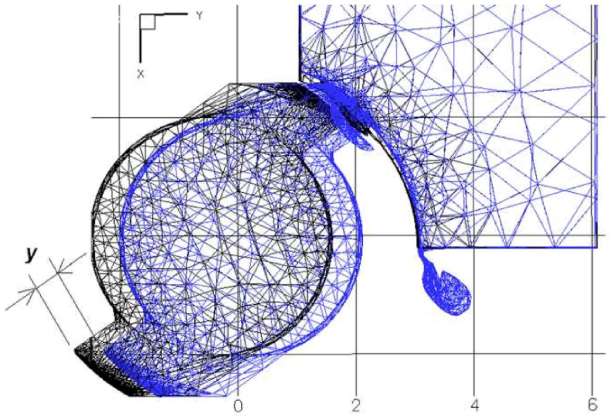

Fig. 13. Model of the cutting process of the Titanium alloy with a plot of finite elements before (blue colour) and after the deformation (black colour)

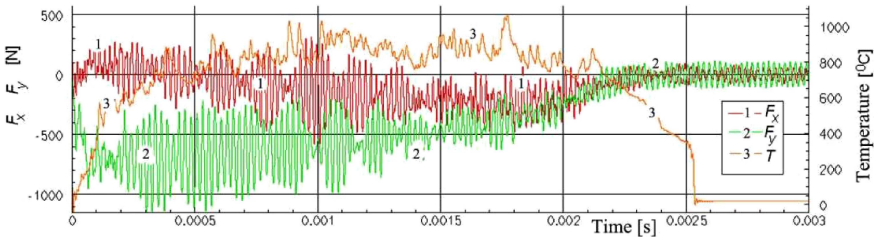

Fig. 14. Graph of the course of the main cutting force components (F_x, F_y)and the maximum temperature of the edge ($T_{\max}$) during down milling of Titanium alloy Ti6Al4V, assuming fully rigid construction of the tool (beam length $L_1 = 0$ mm)

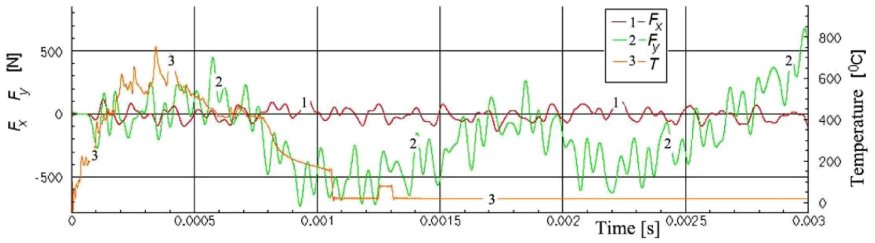

Fig. 15. Graph of the course of the main cutting force components (F_x, F_y) and the maximum temperature of the edge ($T_{\max}$) during down milling of Titanium alloy Ti6Al4V, with the rigidity, determined by the free length of the tool (beam) with length $L_1 = 60$ mm

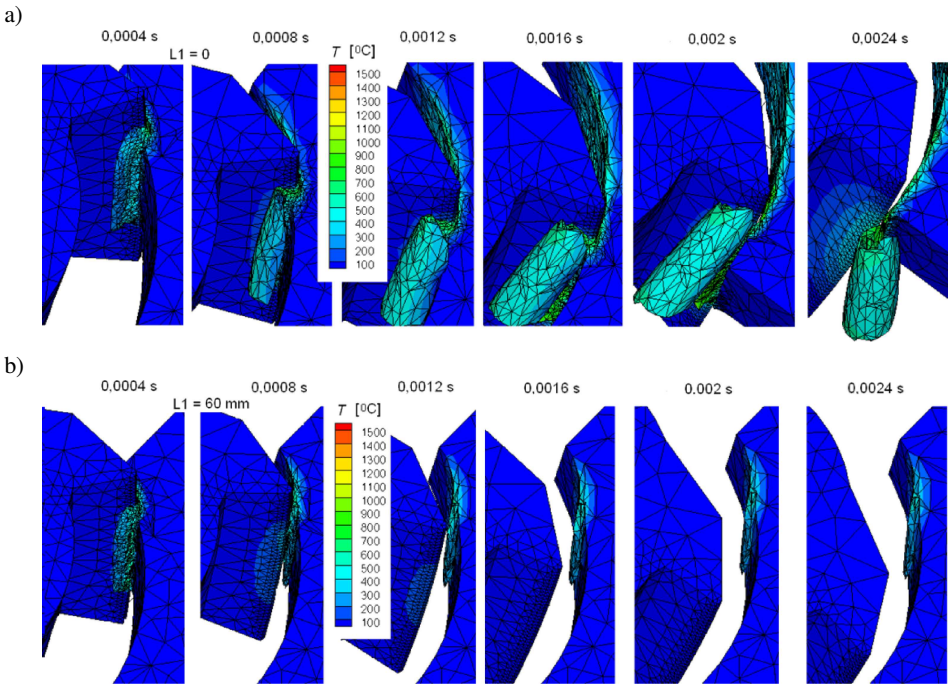

Fig. 16. Subsequent stages of the chip formation during the down milling of Titanium alloy Ti6Al4V in the case of: a) the full rigidity of the tool, b) the rigidity, determined by the free length of the tool (beam) with length $L_1 = 60$ mm

The shape of the finite elements plot is visualized in Figs. 8 and 13 in blue colour, deformed in the degree related to the rigidity of the tool (along with the fastening rigidity in the holder) and the cutting resistance values.

In the model research the down milling process was adopted. This means, that during feeding of the edge inside the work piece material, a cross-section of the machined layer is decreased, causing the gradual decrease of the main cutting force value.

A graph showing the course of the main cutting force components (F_x, F_y, F_z) and the maximum temperature of the edge ($T_{\max}$), assuming fully rigid construction of the tool, is presented in Fig. 9 (machining of the Aluminium alloy) and Fig. 14 (milling of the Titanium alloy).

Taking into account susceptibility of the Tool – Tool Holder system on the effect of the cutting resistance, in accordance with the scheme shown in Figs. 3–4, the graphs of the main cutting force components course during machining of the Aluminium alloy for two different free lengths of the mill: $L_1 = 100$ mm and $L_1 = 200$ mm, (Table 1) is presented in Figs. 10–11; while that during machining of Titanium alloy for the free length of the mill $L_1 = 60$ mm, is presented

Table 2
Differences of the main cutting force component F_y in relations to its value, reached in the case of the full rigidity set (F_{y0}) and the maximum deflection of the tool end ($y_{\max}$). Calculated values

Work piece material	Length of tool L_1 [mm]	Diameter of tool D [mm]	$dF_y = F_y - F_{y0}$ [N]	$y_{\max}$ [mm]
Al6061	0	8	0	0
	100		190	0.22
	200		140	1.3
Ti6Al4V	0	6	0	0
	60		400	0.56

in Fig. 15. We can see large variations of the main cutting force components values, being the consequence of the variability of the machined layer section during the process of the chip formation. A force, acting on the tool edge causes its deformation, and consequently the relative drag of the edge in relation to its planned position, if we assume the fully rigid system. This drag size will seriously depend on the free length of the tool, its diameter (moment of inertia), Young's modulus and the machined material (cutting resistance). In Table 2, the size of maximum deflection of the tool for the model research is collated, in compliance with the parameters presented in Table 1. Variations of the component F_y of the total cutting force are smaller for the greater feeding of the tool from the tool holder. The maximum difference in value of this force (the case of the Aluminium alloy machining), for $L_1 = 200$ mm is $dF_y \sim 140$ N; while for $L_1 = 100$ mm is $dF_y \sim 190$ N. Value of the component cutting force was calculated in accordance with the formula (6). The tool with the longer outreach deforms still more, due to its smaller rigidity

$$dF_y = F_y - F_{y0}, \tag{7}$$

where F_{y0} – value of the cutting force component F_y for the ideal rigid system.

A consequence of the tool susceptibility is the machined layer thickness decrease, in relation to the assumed values (errors of shape) as well as the considerable decline of the machined surface quality (roughness, waviness). A time variable size of the tool deflection from the set position, caused by the variability of the force value, leads to generation of vibrations during the machining process. In the further part of the model research, a simulation of the down milling of Titanium alloy was carried out. This material is much more difficult to machine than the Aluminium alloy, which manifests itself, among other things, with much higher cutting forces generated during the machining. Variations in the component values of the total cutting force reach the level of 400 N (Fig. 15). So considerable cutting forces cause the maximum deformation of the tool tip, approx. 0.56 mm (Fig. 13). So large distance of the cutting edge from the work piece material causes in effect complete loss of contact between the edge and the machined object and interruption of the cutting process (Fig. 16). This in turn, causes the violent drop of the force value, restoring contact between the edge and the machined object, and starts the decohesion process, however with much smaller thickness of the machined layer. In case of the decrease in thickness below the so called minimum thickness of the machined layer, instead of the machining a slippage of the cutting edge on the machined surface can occur.

In Figs. 14–15, we can observe substantial differences in the course of the main cutting force components (F_x, F_y) during the down milling of the Titanium alloy (Ti6Al4V), assuming the fully rigid tool construction, in relation to the tool susceptible to deformations in result of the cutting force. In the second case there is no monotonic decrease of the force value as the machined layer thickness decreases. The forces oscillate around their average values.

3. Conclusions

Modelling of the milling process, with regard to the static rigidity of the tool, allowed us to determine the machining allowance thickness, smaller in relation to the assumed values (errors of shape). The time variable tool deflection size from the set position, caused by the variability of the force value, leads to generation of vibrations in the cutting process, which effects in the considerable decline in quality of the machined surface. This effect is more visible in the case of milling of the difficult to machine material, like the Titanium alloy. It causes the necessity of the rigid cutting tool application, which means the biggest diameter and shortest free length of the tool as possible.

REFERENCES

[1] A.C. Lee, C.S. Liu, and S.T. Chiang, "Analysis of chatter vibration in a cutter-work piece system", *Int. J. Mach. Tools Manufact.* 31 (2), 221–234 (1991)

[2] R. Rusinek, J. Warmiński, and K. Szabelk, *Nonlinear Vibrations in Turning Process,* IZT Publishers, Lublin, 2006, (in Polish).

[3] G. Stépán, "Retarded dynamical systems: stability and characteristic functions", Longman, London, 1989.

[4] J. Tlusty, "Dynamics of high-speed milling", *ASME J. Engin. Indust.* 118, 59–67 (1986).

[5] W. Zębala, "Vibrations influence on the cutting process", *Proc. microCAD 2006 Conf.* 1, 175–180 (2006).

[6] T. Szalay, "Modelling in metal cutting theory", in *Concurrent Product and Technology Development*, ed. B. Barisic, pp. 223, Faculty of Engineering, Rijeka, 2009.

[7] H.Z. Li, X.P. Li, and X.Q. Chen, "A novel chatter stability criterion for the modelling and simulation of the dynamic milling process in the time domain", *Int. J. Adv. Manuf. Technol.* 22, 619–625 (2003)

[8] H.Z. Li and X.P. Li, "Modelling and simulation of chatter in milling using a predictive force model", *Int. J. Mach. Tools Manufact.* 40 (14), 2047–2071 (2000).
[9] R.I. Minis and R. Yanushevsky, "A new theoretical approach for the prediction of machine tool chatter in milling", *ASME J. Engin. Indust.* 115, 1–8 (1993).
[10] S. Smith and J. Tlusty, "Stabilizing chatter by automatic spindle speed regulation", *Annals CIRP* 41 (1), 1–12 (1992).
[11] Y. Altintas and E. Budak, "Analytical prediction of stability lobes in milling", *Annals CIRP* 44 (1), 357–362 (1995).
[12] B. Storch, *The Basis of Machining*, Koszalin University of Technology, Koszalin, 2001, (in Polish).
[13] J. Tlusty and M. Polacek, "The stability of machine tools against self-excited vibrations in machining", *Int. Research in Production Engineering* 1, 465–474 (1963).
[14] R. Ebner, P. Gruber, W. Ecker, O. Kolednik, M. Krobath, and G. Jesner, "Fatique damage mechanisms and damage evolution near cyclically loaded edges", *Bull. Pol. Ac.: Tech.* 58 (2), 267–279 (2010).
[15] W. Ostapski, "Analysis of the stress state in the harmonic drive generator – flexspline system in relation to selected structural parameters and manufacturing deviations", *Bull. Pol. Ac.: Tech.* 58 (4), 683–698 (2010).
[16] *User's Manual of AdvantEdge v5.6 Machining Simulation Software*, Minneapolis, 2010.